Nonlinear laser dynamics induced by frequency shifted optical feedback: application to vibration measurements

Vadim Girardeau, Carolina Goloni, Olivier Jacquin, Olivier Hugon, Mehdi Inglebert, Eric Lacot

Non-linear laser dynamics induced by frequency shifted optical feedback: Application to vibration measurements

VADIM GIRARDEAU,[1] CAROLINA GOLONI,[2] OLIVIER JACQUIN,[1] OLIVIER HUGON,[1] MEHDI INGLEBERT,[1] ERIC LACOT[1,*]

[1]*Univ. Grenoble Alpes, CNRS, LIPhy, F-38000 Grenoble, France*
[2]*Pontifical Univ. Catholic, CETUC, CEP 22453-900 Rio de Janeiro, Brazil*
**Corresponding author: eric.lacot@univ-grenoble-alpes.fr*

Received XX Month XXXX; revised XX Month, XXXX; accepted XX Month XXXX; posted XX Month XXXX (Doc. ID XXXXX); published XX Month XXXX

In this article, we study the non-linear dynamics of a laser subjected to frequency shifted optical reinjection coming back from a vibrating target. More specifically, we study the non-linear dynamical coupling between the carrier and the vibration signal. The present work shows how the non-linear amplification of the vibration spectrum is related to the strength of the carrier and how it must be compensated to obtain accurate (i.e. without bias) vibration measurements. The theoretical predictions, confirmed by numerical simulations, are in good agreement with the experimental data. The main motivation of this study is the understanding of the non-linear response of a LOFI (Laser Optical Feedback Imaging) sensor for quantitative phase measurements of small vibrations, in the case of strong optical feedback. © 2016 Optical Society of America

OCIS codes: *(120.0120) Instrumentation, measurement, and metrology; (120.7280) Vibration analysis; (140.0140) Lasers and laser optics; (140.3430) Laser theory.*

http://dx.doi.org/10.1364/AO.99.0999

1. INTRODUCTION

Laser properties (power, polarization, coherence, dynamical behavior …) can be significantly affected and modified by optical feedback [1,2] which allows for the realization of non-conventional sensors. One potential application is Laser Feedback Interferometry (LFI), where the steady-state intensity of a laser is modified by coherent optical feedback from an external surface. With this phase sensitive technique the signal depends on the reflectivity, distance and motion of the target [3]. However, when the amount of re-injected light is very small, the interference contrast occurring inside the laser cavity is drastically reduced. To overcome this problem, one solution is to use the dynamical properties of the laser which can be several orders of magnitude more sensitive to optical feedback than the laser steady-state properties. Since the pioneering work of K. Otsuka on self-mixing modulation effect in a class-B laser [4], the dynamical sensitivity of lasers to frequency shifted optical feedback has been used in metrology [5], for example in self mixing Laser Doppler Velocimetry (LDV) [6-8] and in Laser Optical Feedback Imaging (LOFI) [9-11]. Compared to conventional optical heterodyne detection, frequency shifted optical feedback allows for higher (several order of magnitude) intensity modulation contrast [12-14].

For weak optical feedback, the laser dynamics is linear and the maximum of the modulation is reached when the shift frequency is resonant with the laser relaxation oscillation frequency. In this condition, an optical feedback level as low as -170 dB (i.e. 10^{17} times weaker than the laser intra-cavity power) has been detected [6].

On the opposite, phase measurements (such as profilometry or vibrometry) with low noise necessitate to increase the amount of optical feedback reinjected inside the laser cavity [15-17]. For strong optical feedbacks, the laser dynamics becomes non-linear, making it difficult to obtain quantitative measurements.

The main objective is to demonstrate the possibility to accurately measure very small vibration amplitudes (i.e. sub-wavelength), from the non-linear dynamics of a laser submitted to a strong frequency-shifted optical feedback. Experimentally, the use of a LOFI set up is motivated by the following reasons: i) the LOFI interferometer is always self-aligned because the laser simultaneously fulfils the functions of the source (i.e. photons-emitter) and of the photo-detector (i.e. photons-receptor); ii) the LOFI detection is shot noise limited (even with a low power laser) in a frequency range located near the relaxation oscillation frequency of the laser [12-14].

This article is organized as follows. In section 2, we firstly recall the equations governing the dynamics of a laser with a frequency-shifted optical reinjection back-scattered from a vibrating target. Then the signal processing to extract vibration measurements from the laser

dynamics is explained. The end of this section is devoted to numerical simulations where we show typical examples of numerical vibration signals (harmonic and transient) extracted from the laser dynamic in both the linear and nonlinear regimes. These numerical simulations show that the gain of the laser dynamics needs to be compensated (and therefore to be known) to extract accurate (i.e. without bias) vibration amplitude. In section 3, a bifurcation analysis is made to obtain an asymptotic solution for the gain of the laser dynamics. Our calculations show that the carrier and the vibration signal are coupled through the non-linear laser dynamics and we demonstrate that the nonlinear amplification of the vibration spectrum is related to the amplitude of the carrier signal. Therefore, our calculation confirms that to obtain quantitative vibration measurements, the non-linear gain must be taken into account in the signal processing. Section 4 is devoted to the measurement of experimental vibrations with a LOFI (Laser Optical Feedback Imaging) setup. The theoretical predictions, confirmed by numerical simulations, are in good agreement with the experimental data. The final section is devoted to the general discussion of these results and to their prospective applications.

2. LASER WITH FREQUENCY-SHIFTED OPTICAL FEEDBACK

A. Basic equations for vibrometry

For weak optical feedback ($R_e << 1$) and a short round trip time delay ($\tau_e << 1/F_e$), the dynamical behavior of a laser with a frequency shifted (F_e) optical feedback can be described by the following set of differential equations [12]:

$$\frac{dI}{dt} = BIN - \gamma_c I + \gamma_c 2\sqrt{R_e} I \cos\left[\Omega_e t + \Phi_e(t)\right] + F_I(t) \quad \textbf{(1a)}$$

$$\frac{dN}{dt} = \gamma_1\left[N_0 - N\right] - BNI \quad \textbf{(1b)}$$

$$\left\langle F_I(t)\right\rangle = 0 \quad \textbf{(1c)}$$

$$\left\langle F_I(t) F_I(t-\tau)\right\rangle = 2\gamma_c \left\langle I\right\rangle \delta(\tau) \quad \textbf{(1d)}$$

where I and N are respectively the laser intensity (photon unit) and the population inversion (atom unit). γ_1 is the decay rate of the population inversion, γ_c is the laser cavity decay rate, $\gamma_1 N_0$ is the pumping rate and B is related to the Einstein coefficient (i.e. the laser transition cross section). Regarding the noise, the laser quantum fluctuations are described by the Langevin noise function $F_I(t)$, with a zero mean value and a white noise type correlation function [18,19].

In Eqs. (1), the cosine function expresses the coherent interaction (i.e. the beating at the angular frequency: $\Omega_e = 2\pi F_e$) between the lasing and the feedback electric field. The optical reinjection back-scattered from a vibrating target is characterized by the effective power reflectivity R_e and the time dependent optical phase shift $\Phi_e(t) = \frac{2\pi}{\lambda_c} 2 d_e(t)$ induced by the distance $d_e(t)$ between the laser and the vibrating target. λ_c is the laser wavelength.

In the absence of optical feedback ($R_e = 0$), the laser steady-state is given by the mean values of the population inversion and of the laser intensity:

$$N_S = \gamma_c / B, \quad \textbf{(2a)}$$

$$I_S = I_{sat}\left[\eta - 1\right], \quad \textbf{(2b)}$$

where $\eta = N_0/N_S$ is the normalized pumping parameter and $I_{sat} = \gamma_1/B$ is related to the saturation intensity of the laser transition. Also for $R_e = 0$, the intrinsic dynamics of a class-B laser ($\gamma_c >> \gamma_1\eta$) is characterized by damped relaxation oscillations of the laser output power with a relaxation angular frequency $\Omega_R = \sqrt{\gamma_1\gamma_c(\eta - 1)}$ and a damping rate $\Gamma_R = \gamma_1\eta/2$. Experimentally, this transient dynamics is constantly excited by the laser quantum noise described by the Langevin force $F_I(t)$.

In the presence of optical feedback ($R_e \neq 0$), the laser intrinsic dynamics can be modified and the extent of changes in the laser dynamical properties depends on the feedback conditions (R_e, Ω_e). In this article, we call "*strong feedback*", the situation where the modulation frequency is nearly resonant ($\Omega_e \approx \Omega_R$) and where the amount of optical feedback is high enough to induce non-linear dynamical behaviors in the laser output power modulation. The strong feedback situation is also characterized by a strong modification of the RF signal power spectrum of the laser [20, 21]. In particular, the relaxation oscillations frequency can decrease, jointly with a modification of the shape of the RF noise power spectrum of the laser [22]. In contrast, the *"weak feedback"* regime corresponds to the situation where the modulation frequency is far away from the resonance ($\left|\Omega_e - \Omega_R\right| >> 0$) and where the amount of optical feedback (R_e) is small enough to induce only linear dynamical behavior in the laser output power modulation. In this situation, the RF noise power spectrum of the laser, with and without optical feedback, is unchanged. Here, let us mentioned that the RF noise power spectrum is an image of the gain (i.e. of the modulation transfer function) of the laser dynamics [22]. As explained in the following section, the knowledge of this gain is of paramount importance to extract accurate (i.e. without bias) vibration measurements from the laser dynamics of a reinjected laser.

B. Signal processing for vibrometry

The aim of the present paper is to explain how it is possible to extract the time dependence of the phase shift of the optical feedback, namely $\Phi_e(t)$ (and consequently $d_e(t)$) from the laser dynamics, in both the weak and the strong feedback regimes.

For a laser with frequency shifted optical feedback, the output power modulation of the laser is given by the convolution product (symbol $\otimes$) between the input modulation (i.e. the coherent beating at the carrier frequency) and the impulse response of the laser dynamics which is the is inverse of the Fourier transform (FT^{-1}) of the gain of the laser dynamics $G(\Omega, R_e, \Omega_e)$ (i.e. of the modulation transfer function):

$$\Delta I(t) = I(t) - I_s \propto \sqrt{R_e} \times \left[FT^{-1}\left[G(\Omega, R_e, \Omega_e)\right] \otimes \exp\left[i\left(\Omega_e t + \Phi_e(t)\right)\right] + cc\right] \quad \textbf{(3)}$$

In Eq. (3), one can notice that the gain of the laser dynamics $G(\Omega, R_e, \Omega_e)$ depend on the feedback condition (R_e, Ω_e). Principally in the strong feedback regime.

To extract the temporal evolution of the phase induced by the vibration ($\Phi_e(t)$), the different steps of the signal processing are given by the set of Eqs. (4a-f):

$$FT\left[\Delta I(t)\right] \propto \left\{ \begin{array}{l} \left\{ \begin{array}{l} \sqrt{R_e} G(\Omega, R_e, \Omega_e) \\ \times \left[FT\left[\exp\left(+i\Phi_e(t)\right)\right] \otimes \delta(\Omega - \Omega_e) \right] \end{array} \right\} \\ + \left\{ \begin{array}{l} \sqrt{R_e} G^*(\Omega, R_e, \Omega_e) \\ \times \left[FT\left[\exp\left(-i\Phi_e(t)\right)\right] \otimes \delta(\Omega + \Omega_e) \right] \end{array} \right\} \end{array} \right\}, \quad \textbf{(4a)}$$

$$FT_{\Delta\Omega_e}\left[\Delta I(t)\right] \propto \left\{ \begin{array}{l} \sqrt{R_e}\, G(\Omega, R_e, \Omega_e) \\ \times \left[FT\left[\exp\left(+i\Phi_e(t)\right)\right] \otimes \delta(\Omega - \Omega_e) \right] \end{array} \right\}, \quad \textbf{(4b)}$$

$$\frac{FT_{\Delta\Omega_e}\left[\Delta I(t)\right]}{G(\Omega, R_e, \Omega_e)} \propto \sqrt{R_e} \left\{ \left[FT\left[\exp\left(+i\Phi_e(t)\right)\right] \otimes \delta(\Omega - \Omega_e) \right] \right\}, \quad \textbf{(4c)}$$

$$FT^{-1}\left[\frac{FT_{\Delta\Omega_e}\left[\Delta I(t)\right]}{G(\Omega, R_e, \Omega_e)} \right] \propto \sqrt{R_e} \left\{ \exp\left(+i\Phi_e(t)\right) \exp\left(+i\Omega_e t\right) \right\}, \quad \textbf{(4d)}$$

$$\left[FT^{-1}\left[\frac{FT_{\Delta\Omega_e}\left[\Delta I(t)\right]}{G(\Omega, R_e, \Omega_e)} \right] \right] \exp\left(-i\Omega_e t\right) \propto \sqrt{R_e} \left\{ \exp\left(+i\Phi_e(t)\right) \right\}, \quad \textbf{(4e)}$$

$$\arg\left[\left[FT^{-1}\left[\frac{FT_{\Delta\Omega_e}\left[\Delta I(t)\right]}{G(\Omega, R_e, \Omega_e)} \right] \right] \exp\left(-i\Omega_e t\right) \right] = \Phi_e(t). \quad \textbf{(4f)}$$

Fisrtly [Eq. (4a)], the Fourier Transform of the time evolution of the laser output power is calculated. Then [Eq. (4b)], the Fourier spectrum is filtered using a bandpass filter with a central frequency Ω_e and a bandwidth $\Delta\Omega_e$. The bandwidth is adapted to the frequency range of the vibration spectrum. Thirdly [Eq. (4c)], the distortion of the vibration spectrum induced by the laser dynamics (i.e. the amplification gain) is compensated. Then, coming back to the temporal space [Eq. (4d)], the signal is demodulated [Eq. (4e)] and finally [Eq. (4f)], the temporal evolution of the phase is extracted from the complex signal.

In this signal processing, it can be noticed that the multiplication, by any real constant number, of the input signal (i.e. the laser output power modulation) , has no impact on the extraction of output signal, which is a phase signal. So, the gain can be multiplied by any real constant. Therefore, for the experimental measurement of vibrations, the absolute knowledge of the amplitude of the gain is not necessary (i.e. only the complex frequency shape is important). This is due to the fact that, for vibration measurements, only the relative ratio between the amplitudes of the spectral components is important.

C. Compensation of the gain of the laser dynamics

To demonstrate how different kinds of vibrations can be extracted from the laser dynamics, we have numerically solved the set of differential equations given by (1).

1. Numerical harmonics vibrations

Fig. 1 shows examples of the calculations of a harmonic vibration:

$$\Phi_e(t) = \Phi_a \sin\left(\Omega_a t\right), \quad \textbf{(5)}$$

with an acoustic angular frequency $\Omega_a = \Omega_R / 3.5$ and with a small vibration amplitude $\Phi_a = 2\pi/50$. The calculations are made for a given frequency shift ($\Omega_e = 1.1\Omega_R$) and for two optical feedback reflectivities ($R_e = 10^{-9}$ and $R_e = 10^{-7}$).

Figs 1a-b show the signal is principally composed of one peak at the carrier frequency (Ω_e) and two peaks for the vibration sidebands ($\Omega_e \pm \Omega_a$). When the feedback is weak ($R_e = 10^{-9}$), one can see in Fig. 1a, that the complex gain adjusted on the noise power spectrum exhibits only one resonance (i.e. is linear). On the other hand, when the feedback is strong ($R_e = 10^{-7}$), the gain, which becomes non-linear, exhibits two resonances symmetrically located on both sides of the carrier frequency (Fig. 1b) [22]. As already mentioned the RF noise power spectrum is an image of the gain (i.e. of the modulation transfer function) of the laser dynamics [22] and therefore helps to obtain it as it is explained in the theoretical section (i.e. section III).

In both cases, the middle row (Figs. 1c and 1d) show a comparison between the exact vibration motion and the vibration obtained after the signal processing, but without the gain compensation (i.e. without the signal processing step given by Eq. (4c)). One can see that neither the amplitude nor the phase of the detected vibration is good. In the weak feedback case, the carrier signal, which is near the resonance, is amplified much more than the vibration sidebands and thus the vibration amplitude is lower than the real one. In the strong feedback case the opposite situation occurs. The vibration sidebands which are near the resonances are much more amplified than the carrier signal, and therefore the detected vibration amplitude is larger than the real one. In both cases, one can also notice a π phase-shift induced by the resonance.

Finally, the lower traces (Figs 1e and 1f) show that the accurate vibration is recovered in both cases (weak or strong feedback) if the complex gain compensation (i.e. if the division by $G(\Omega, R_e, \Omega_e)$) is made in the signal processing. So, Fig. 1 clearly shows that the gain compensation (linear or non-linear) is necessary to obtain accurate (i.e. without bias) quantitative vibration measurements (amplitude and phase) from the reinjected laser dynamics.

The comparison of Figs. 1e and 1f also shows that the vibration amplitude is better recovered when the amount of optical feedback increases. This effect is principally due to the increase of all the vibration components relatively to the noise baseline. So, even if for a strong optical feedback, the laser dynamics becomes non-linear (i.e. much more complicated), the compensation of the non-linear amplification allows to restore vibration measurement with an

improved accuracy. Indeed, the standard deviation of the difference between the exact vibration and the extracted vibration is equal to $0.02\,rad\ \left(\approx 2\pi/300\right)$ for $R_e = 10^{-9}$ (left column) and equals to $0.01\,rad\ \left(\approx 2\pi/600\right)$ for $R_e = 10^{-7}$ (right column).

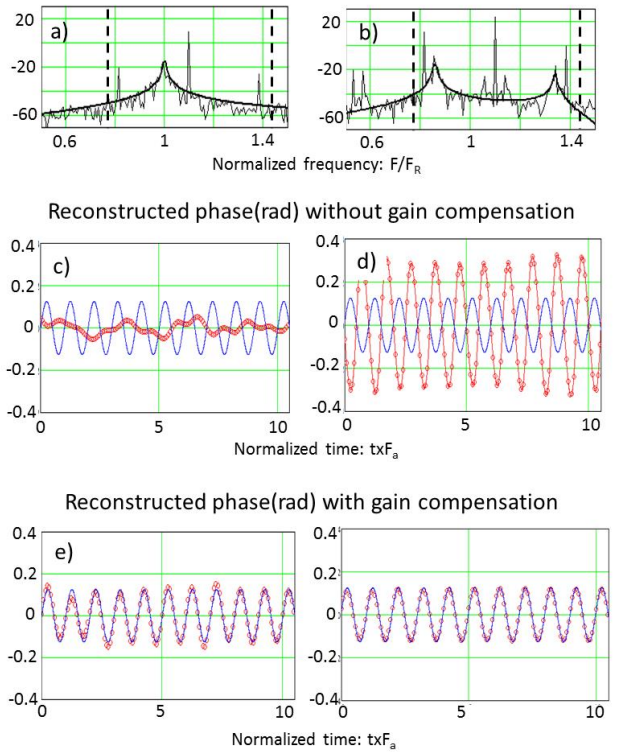

Fig. 1: Numerical simulation. Calculations of a harmonic vibration ($\Omega_a = \Omega_R/3.5$) with a small amplitude of vibration ($\Phi_a = 2\pi/50$). The left column (a, c, e) corresponds to a weak optical feedback ($R_e = 10^{-9}$) while the right one (b, d, f) corresponds to a strong optical feedback ($R_e = 10^{-7}$). The top row (a, b) shows the laser power spectrum where the resonance gain (bold line) is adjusted on the noise spectrum. The calculations are made with $\Omega_e = 1.1\Omega_R$ and a bandpass filter $\Delta\Omega_e = \Omega_R/1.5$ (see dashed vertical lines). The middle row (c, d) shows a comparison between the exact vibration motion (solid line) and the vibration obtained after the signal processing (line of circles), but without the gain compensation. The bottom row (e, f) shows the same comparison when the gain compensation has been applied. Laser parameters: $\eta = 1.2$, $\gamma_1/\gamma_c = 1\times10^{-5}$, $F_R/\gamma_c = 2.251\times10^{-4}$.

2. Numerical transient vibrations

To verify that our signal processing can be applied to any kinds of vibrations, we have numerically simulated transient vibrations:

$$\Phi_e(t) = \frac{\Phi_a}{1+\left(\dfrac{t-\tau}{\tau_a}\right)^2}, \qquad \textbf{(6)}$$

with a half time width $\tau_a \approx 1.8/F_R$ (i.e. a broad spectral bandwidth $\Delta\Omega_a \approx \Omega_R/1.8$) and a time delay $\tau = 16.4\,\tau_a$. Fig. 2 shows examples of the extraction of an impulse vibrations for 3 different values of the amplitudes ($\Phi_a = 2\pi/5$, $\Phi_a = 2\pi/50$ and $\Phi_a = 2\pi/500$). The numerical simulations have been made for a given frequency shift ($\Omega_e = 1.1\Omega_R$) and for strong feedback reflectivity ($R_e = 10^{-7}$).

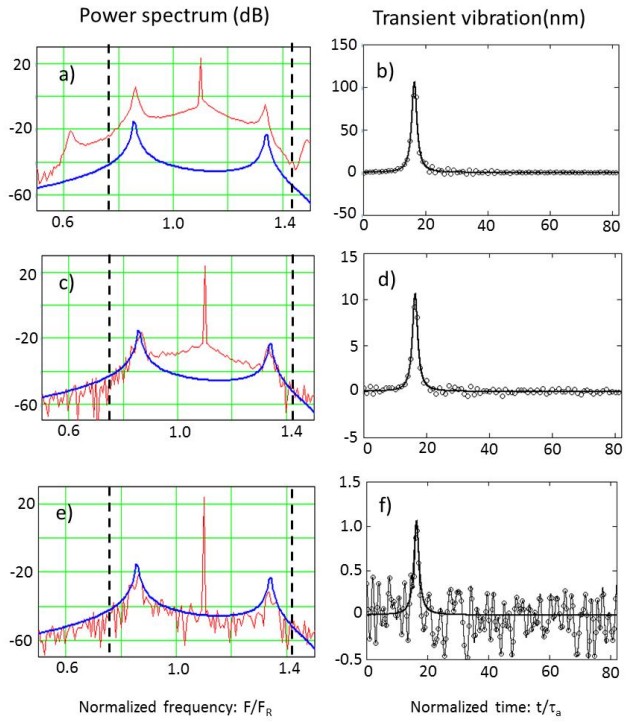

Fig. 2: Numerical simulation. Calculations of a transient vibration with a half time width ($\tau_a \approx 1.8/F_R$) and a time delay ($\tau = 16.3\,\tau_a$). Top row (a,b): large amplitude of vibration ($\Phi_a = 2\pi/5$). Middle row (c, d): small amplitude of vibration ($\Phi_a = 2\pi/50$). Bottom row (e,f): very small amplitude of vibration ($\Phi_a = 2\pi/500$). The left column (a, c, e) shows the RF power spectra, where the bold lines show the shape of the non-linear gain used for the signal processing. The right column (b, d, f) shows a comparison between the exact vibration motion (solid line) and the vibration obtained after the signal processing (circles). All the calculations are made with the same feedback conditions ($\Omega_e = 1.1\Omega_R$ and $R_e = 1\times10^{-7}$) and the same bandpass filter $\Delta\Omega_e = \Omega_R/1.5$ (corresponding to the dashed vertical lines). Laser parameters: see Fig. 1.

Firstly, one can notice on the left column, that the non-linear gain used for the gain compensation in the signal processing, is always the same and is also identical to the one used in Fig. 1 (right column) for the calculation of harmonic vibration. This is due to the fact that the feedback conditions are the same and consequently the gain of the laser dynamics $G\left(\Omega, R_e, \Omega_e\right)$ is the same for all these vibration calculations. Secondly, the right column shows that impulse vibration with an accurate amplitude and an accurate time delay can be extracted from the non-linear laser dynamics (Figs. 2b , 2d, and 2f). Thirdly, the impulse shape is recovered regardless of the vibration amplitude, even when the vibration amplitude is large (see Figs. 2a and b) and when the RF power spectrum is strongly perturbed by non-linear dynamical effects of higher order. Finally, on Fig. 2f, an amplitude

of $d_a = 1 \pm 0.2\ nm \approx \lambda/1000$ is detected, showing the high potential of this measurement method for the detection of small vibration amplitudes at relatively high frequencies. It must be noted that the SNR of the order of 5 has been obtained with a filtering process (see Eq. 4b) adapted to the width of the vibration spectrum ($\Delta\Omega_e = \Omega_R/1.5 \approx \Delta\Omega_a$).

For a narrower bandwidth ($\Delta\Omega_e < \Delta\Omega_a$) the noise (i.e. the fluctuation at the base of the impulse vibration) is lower, but the vibration spectrum is truncated. Consequently, the shape (amplitude and width) of the reconstructed vibration pulse is not the good one.

Conversely if the bandwidth is wider ($\Delta\Omega_e > \Delta\Omega_a$), the noise increases, without any significant improvement of the reconstructed pulse shape. Therefore, with the non-linear gain compensation, the detection of very small vibration amplitudes ($\Phi_a = 2\pi/500$) seems to be possible with a reinjected laser.

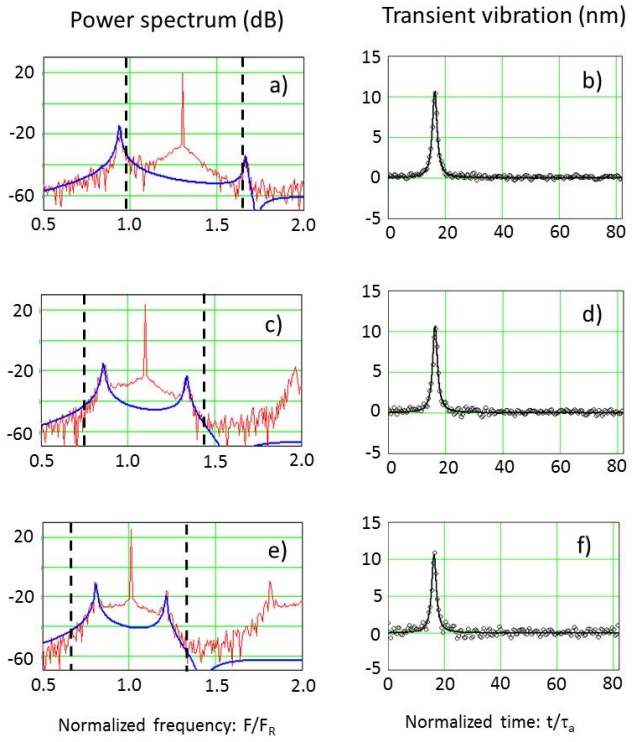

Fig. 3: Numerical simulation. Calculations of a transient vibration with a full time width $\tau_a \approx 1.8/F_R$, a time delay $\tau = 16.3\tau_a$ and a vibration amplitude $\Phi_a = 2\pi/50$. The measurements are made with the same feedback reflectivity $R_e = 1\times10^{-7}$ but for different values of the carrier frequency (F_e) Top row (a, b): $F_e/F_R = 1.3$; Middle row (c, d): $F_e/F_R = 1.1$; Bottom row (e, f): $F_e/F_R = 1.01$. The left column (a, c, e) shows the RF power spectra, where the bold lines show the shape of the non-linear gain used for the signal processing. The right column (b, d, f): shows a comparison between the exact vibration motion (solid line) and the vibration obtained after the signal processing (circles). All the calculations are made with the same bandpass filter $\Delta\Omega_e = \Omega_R/1.5$ (corresponding to the dashed vertical lines). Laser parameters: see Fig. 1.

In Fig. 3, the transient vibration is again a short impulse vibration with a wide spectral bandwidth ($\Delta\Omega_a = \Omega_R/1.8$) and with a small vibration amplitude ($\Phi_a = 2\pi/50$), but now the calculations have been made for a strong feedback reflectivity ($R_e = 10^{-7}$) and for 3 different values of the carrier frequency ($\Omega_e/\Omega_R = 1.3$, $\Omega_e/\Omega_R = 1.1$, and $\Omega_e/\Omega_R = 1.01$).

The left column shows how the non-linear gain (adjusted on the noise power spectrum) is modified when the carrier frequency approaches the intrinsic laser relaxation frequency (i.e. when $\Omega_e/\Omega_R \to 1$). As already mentioned, the modification of the non-linear gain is induced by the modification of the carrier amplitude [22].

One can observe on the left column that the frequency distance between the two maxima (located symmetrically on both sides of the carrier frequency) decreases. Secondly, one can also observe that the amplitude of the maximum located on the right side of the carrier frequency increases in agreement with [22].

The right column of Fig. 3 shows that regardless of the shape of the non-linear gain (i.e. of the frequency shift Ω_e) the impulse vibration is recovered with an accurate amplitude and an accurate time delay. Nevertheless, one can notice a small degradation of the signal to noise ratio (roughly by a factor 2) when $\Omega_e = 1.01\Omega_R$. In Fig. 3f, the higher noise, which is visible at the base of the feet of the impulse vibration, can be attributed to the fact that the adjustment of the noise power spectrum by the non-linear gain is not always perfect and that the amount of noise initially present (i.e. before the gain compensation) inside the bandwidth filter increases when $\Omega_e/\Omega_R \to 1$ (see Fig. 3e).

3. GAIN OF THE NONLINEAR LASER DYNAMICS

As explained in the previous section, accurate (i.e. without bias) vibration measurements are possible with frequency shifted optical feedback in laser, if the gain compensation is applied in the signal processing. So the gain of the laser dynamics needs to be known. The aim of the present section is to obtain an analytic expression of the complex gain $G(\Omega, R_e, \Omega_e)$, whatever the feedback condition (weak or strong) is and therefore whatever the laser dynamics (linear or nonlinear) is.

A. Asymptotic solution for the nonlinear gain

To analytically study the dynamical response of a laser subjected to frequency-shifted optical feedback ($R_e \neq 0$), we have used the asymptotic equation given in [22-24]:

$$\frac{dA}{ds} = -i\left[\sigma_e - 1\right]A - i\frac{A^2A^*}{6} - \frac{\eta\varepsilon}{2}A + i\frac{\delta_e}{4}\exp\left(i\Phi_e\right), \qquad (7)$$

where A is the complex amplitude of the small periodic oscillation and where $\sigma_e = \Omega_e/\Omega_R$ and $s = \Omega_R t$ are respectively the frequency-shift and the time normalized by the relaxation frequency. For our microchip laser, $\varepsilon = \gamma_1/\Omega_R \approx 10^{-3}$ is a small quantity, which allows the use of the asymptotic analysis detailed in [22-24]. In Eq. (7), the optical feedback is described by $\delta_e = 2\sqrt{R_e}\gamma_c/\Omega_R$ and by the optical phase-shift Φ_e .

To obtain the gain (i.e. the modulation transfer function) of the laser dynamic, we now investigate the solutions of Eq. (7), in the particular situation of a vibrating target with a harmonic oscillation:

$$\Phi_e(s) = \Phi_0 + \Phi_a \sin(\sigma_a s + \phi_a), \quad \textbf{(8)}$$

where $\sigma_a = \frac{\Omega_a}{\Omega_R}$ is the normalized acoustic vibration angular frequency, $\Phi_a = \frac{2\pi}{\lambda} 2d_a$ is the phase-shift linked to the vibration amplitude d_a, ϕ_a the modulation phase shift and Φ_0 an additional phase shift corresponding to the mean distance between the laser and the vibrating target. Without loss of generality, we assume: $\Phi_0 = m2\pi$, where m is an integer.

In the case of sub-wavelength vibration amplitudes (i.e. $\Phi_a << 2\pi$), Eq. (7) can be rewritten:

$$\frac{dA}{ds} = -i[\sigma_e - 1]A - \frac{\eta\varepsilon}{2}A - i\frac{A^2 A^*}{6} + i\frac{\delta_e}{4}\begin{bmatrix} J_0(\Phi_a) \\ +J_1(\Phi_a)\exp[i(\sigma_a s + \phi_a)] \\ +J_{-1}(\Phi_a)\exp[i(-\sigma_a s - \phi_a)] \end{bmatrix}, \quad \textbf{(9)}$$

where $J_n(\Phi_a)$ is the Bessel function of the first kind and of order n with: $J_0(\Phi_a) \approx 1$, $J_1(\Phi_a) \approx \Phi_a/2$ and $J_{-1}(\Phi_a) = -J_1(\Phi_a)$.

In the present study, the key term is the cubic one $(-iA^2A^*/6)$ which couples the amplitude of the modulation at the carrier frequency (Ω_e) with the vibration amplitudes at the acoustic sideband frequencies ($\Omega_e \pm \Omega_a$).
The solution of Eq. (9) can be written as:

$$A(s) = C_e + T_R(s) + R_a \exp[i(\sigma_a s + \phi_a)] + L_a \exp[-i(\sigma_a s + \phi_a)], \quad \textbf{(10)}$$

where C_e is the stationary modulation amplitude at the carrier frequency, $T_R(s)$ is the transient dynamics of random excitations (due to quantum noise) around the stationary solution, while R_a and L_a are respectively the amplitudes of the right and left sidebands of the acoustic vibration. One can notice that in Eq. (10), the carrier signal (C_e) has already be studied in [23] and more particularly the hysteresis phenomenon induced by the periodic modulation, while the noise power spectrum (T_R) and more particularly the shift of the laser relaxation frequency has already been studied in [22]. The aim of the present paper is focused on the study the complex vibration sidebands (R_a and L_a) and how they are amplified by the laser dynamics, in order to be able to restore accurate vibration measurements.
In the forthcoming study, we assume that the carrier signal is much stronger than the laser quantum noise and the vibration sidebands (i.e. $|C_e| >> |T_R(s)|, |R_a|, |L_a|$). Keeping only the first order non-linear terms, Eq. (10) gives:

$$\begin{aligned} A^2A^* \approx\ & C_e C_e C_e^* \\ & + 2C_e C_e^* T_R + C_e C_e T_R^* \\ & + \left[2C_e C_e^* R_a + C_e C_e L_a^*\right]\exp[+i(\sigma_a s + \phi_a)] \\ & + \left[2C_e C_e^* L_a + C_e C_e R_a^*\right]\exp[-i(\sigma_a s + \phi_a)] \end{aligned} \quad \textbf{(11)}$$

Inserting Eqs.(10) and (11) into Eq. (9) gives the following equalities:

$$i(\sigma_e - 1)C_e + i\frac{C_e^2 C_e^*}{6} + \frac{\eta\varepsilon}{2}C_e = i\frac{\delta_e}{4}J_0(\Phi_a), \quad \textbf{(12a)}$$

$$\frac{dT_R}{ds} = -\left[\frac{\eta\varepsilon}{2} + i(\sigma_e - 1) + i\frac{C_e C_e^*}{3}\right]T_R - i\frac{C_e^2}{6}T_R^*, \quad \textbf{(12b)}$$

$$R_a\left[\frac{\eta\varepsilon}{2} + i\sigma_a + i(\sigma_e - 1) + i\frac{C_e C_e^*}{3}\right] + L_a^*\left[i\frac{C_e C_e}{6}\right], = i\frac{\delta_e}{4}J_1(\Phi_a) \quad \textbf{(12c)}$$

$$R_a^*\left[i\frac{C_e C_e}{6}\right] + L_a\left[\frac{\eta\varepsilon}{2} - i\sigma_a + i(\sigma_e - 1) + i\frac{C_e C_e^*}{3}\right], = i\frac{\delta_e}{4}J_{-1}(\Phi_a) \quad \textbf{(12d)}$$

Eqs. (12a-b) have been already studied in [22,23]. Let us recall that the analytical resolution of Eq. (12a) shows that the power spectrum of the output power modulation at the carrier frequency ($|C_e(\delta_e, \sigma_e)|^2$ versus σ_e) exhibits hysteresis in the strong feedback situation and that the extent of the hysteresis zone increases with the amount of optical feedback δ_e [22, 23, 25, 26]. Jointly, the study of the transient dynamics [Eq. (12b)] allows to determine the noise power spectrum of the laser submitted to frequency shifted optical feedback. Let us recall that the noise power spectrum is composed of two resonant curves with a resonant width $\eta\varepsilon$ and with resonance frequencies symmetrically located on both sides of the carrier frequency [22]:

$$\sigma_{R\pm}(\delta_e, \sigma_e) = \sigma_e \pm \delta_R(\delta_e, \sigma_e), \quad \textbf{(13a)}$$

with the detuning:

$$\delta_R(\delta_e, \sigma_e) = \sqrt{\left(\sigma_e - 1 + \frac{|C_e(\delta_e, \sigma_e)|^2}{3}\right)^2 - \left(\frac{|C_e(\delta_e, \sigma_e)|^2}{6}\right)^2}. \quad \textbf{(13b)}$$

Eq. (13) shows that the modification of the noise power spectrum is linked to the strength of the optical feedback (δ_e, σ_e) principally through its dependence on the non-linear modulation amplitude $C_e(\delta_e, \sigma_e)$.

For the vibration, Eqs (12c-d) clearly show that R_a and L_a are coupled through the non-linear modulation amplitude C_e. Nevertheless, the resolution of Eqs (12c-d) is straightforward and gives the following solutions for the modulation amplitude of the two sidebands:

$$R_a(\sigma_a,\delta_e,\sigma_e)=$$

$$\frac{i\frac{\delta_e}{4}J_1(\Phi_a)\left[\frac{\eta\varepsilon}{2}-i\sigma_a+i(\sigma_e-1)+i\frac{|C_e(\delta_e,\sigma_e)|^2}{3}\right]^*-\left(i\frac{\delta_e}{4}J_{-1}(\Phi_a)\right)^*\left[i\frac{C_e(\delta_e,\sigma_e)^2}{6}\right]}{\left[\frac{\eta\varepsilon}{2}+i\sigma_a+i(\sigma_e-1)+i\frac{|C_e(\delta_e,\sigma_e)|^2}{3}\right]\left[\frac{\eta\varepsilon}{2}-i\sigma_a+i(\sigma_e-1)+i\frac{|C_e(\delta_e,\sigma_e)|^2}{3}\right]^*-\left[\frac{|C_e(\delta_e,\sigma_e)|^2}{6}\right]^2}, \quad \textbf{(14a)}$$

$$L_a(\sigma_a,\delta_e,\sigma_e)=$$

$$\frac{i\frac{\delta_e}{4}J_{-1}(\Phi_a)\left[\frac{\eta\varepsilon}{2}+i\sigma_a+i(\sigma_e-1)+i\frac{|C(\delta_e,\sigma_e)|^2}{3}\right]^*-\left(i\frac{\delta_e}{4}J_1(\Phi_a)\right)^*\left[i\frac{C(\delta_e,\sigma_e)^2}{6}\right]}{\left[\frac{\eta\varepsilon}{2}-i\sigma_a+i(\sigma_e-1)+i\frac{|C(\delta_e,\sigma_e)|^2}{3}\right]\left[\frac{\eta\varepsilon}{2}+i\sigma_a+i(\sigma_e-1)+i\frac{|C(\delta_e,\sigma_e)|^2}{3}\right]^*-\left[\frac{|C(\delta_e,\sigma_e)|^2}{6}\right]^2}. \quad \textbf{(14b)}$$

The aim of the following section is to explain why it is possible to extract an accurate (i.e. without a bias) value of Φ_a (and, finally, of the vibration amplitude d_a) from the measurement of the two vibration sidebands (R_a and L_a) conjointly with the carrier modulation (C_e).

Using the two vibration sidebands given by Eqs (14a-b), we define the nonlinear gain of the laser dynamics by the following equation:

$$G(\sigma_v,\delta_e,\sigma_e)=\begin{cases}\dfrac{R_a(\sigma_v-\sigma_e,\delta_e,\sigma_e)}{J_1(\Phi_a)\sqrt{R_e}} & if \quad \sigma_v\geq\sigma_e\\ \dfrac{L_a(\sigma_e-\sigma_v,\delta_e,\sigma_e)}{J_1(\Phi_a)\sqrt{R_e}} & if \quad \sigma_v<\sigma_e\end{cases} \textbf{.(15)}$$

Like the noise power spectrum, this gain exhibits two resonance frequencies symmetrically located on both sides of the carrier frequency [Eqs (13a-b)]. This double resonance is due to the cross coupling between the vibration sidebands.
The frequency distance and the amplitude ratio between the two maxima depend on the feedback conditions and are roughly given by [22]:

$$2\delta_R(\delta_e,\sigma_e)\approx 2\left[\sigma_e-1+\frac{|C_e(\delta_e,\sigma_e)|^2}{3}\right], \quad \textbf{(16a)}$$

$$\frac{|G(\sigma_e+\delta_R,\delta_e,\sigma_e)|}{|G(\sigma_e-\delta_R,\delta_e,\sigma_e)|}\approx\frac{|C_e(\delta_e,\sigma_e)|^2/6}{2\delta_R(\delta_e,\sigma_e)}. \quad \textbf{(16b)}$$

In agreement with the results shown on Figs. 1a-b, Eq. (16b) explains that the amplitudes of the two maxima (located symmetrically on both sides of the carrier frequency) are of the same order of magnitude for strong optical feedback (i.e when $|C_e(\delta_e,\sigma_e)|^2\approx 1$) and that, the right maximum disappears for weak optical feedback $|C_e(\delta_e,\sigma_e)|^2<<1$, leading to the conventional LOFI linear gain, with only one resonance frequency (Ω_R) [12-14]:

$$|G(\sigma_v,\delta_e,\sigma_e)|\underset{|C_e|^2\to 0}{\approx}|G_L(\sigma_v)|==\frac{\frac{\delta_e}{4\sqrt{R_e}}}{\sqrt{(\sigma_v-1)^2+\left(\frac{\eta\varepsilon}{2}\right)^2}} \textbf{. (17)}$$

$$|G_L(\Omega_v)|=\frac{\frac{\gamma_c}{4}}{\sqrt{(\Omega_v-\Omega_R)^2+\left(\frac{\eta\gamma_1}{2}\right)^2}}$$

At this point, one can notice that the linear gain depends only on the intrinsic dynamical parameters of the laser (γ_1, γ_c and η), while the non-linear gain also depends on the feedback conditions (R_e and Ω_e). In agreement with the results shown on Figs. 3a, 3c and 3e, Eqs. (16a-b) allows explaining why the frequency distances between the two maxima decreases and why the amplitude of the maximum located on the right side of the carrier frequency increases, when $\sigma_e=\Omega_e/\Omega_R\to 1$.

C. Gain compensation for vibration measurement

Using Eqs. (12a), (14) and (15), one also obtains:

$$C_e(\delta_e,\sigma_e)=G(\sigma_v=\sigma_e,\delta_e,\sigma_e)J_0(\Phi_a)\sqrt{R_e}. \quad \textbf{(18)}$$

Eqs. (15) and (18) clearly show that an accurate measurement of the vibration can be extracted from the non-linear laser dynamics (C_e, R_a, and L_a), if the non-linear amplification (via G) is compensated:

$$\frac{J_1(\Phi_a)}{J_0(\Phi_a)}=\frac{R_a(\sigma_a,\delta_e,\sigma_e)}{C_e(\delta_e,\sigma_e)}\frac{G(\sigma_v=\sigma_e,\delta_e,\sigma_e)}{G(\sigma_v=\sigma_e+\sigma_a,\delta_e,\sigma_e)}, \quad \textbf{(19a)}$$

$$\frac{J_{-1}(\Phi_a)}{J_0(\Phi_a)}=\frac{L_a(\sigma_a,\delta_e,\sigma_e)}{C_e(\delta_e,\sigma_e)}\frac{G(\sigma_v=\sigma_e,\delta_e,\sigma_e)}{G(\sigma_v=\sigma_e-\sigma_a,\delta_e,\sigma_e)}. \quad \textbf{(19b)}$$

At this point knowing the accurate ratio between the Bessel functions, one could determine Φ_a.

For example, let us recall that for a very small vibration amplitude (i.e. $\Phi_a << 2\pi$) these ratios are equal to: $J_1(\Phi_a)/J_0(\Phi_a) \approx \Phi_a/2$ and $J_{-1}(\Phi_a)/J_0(\Phi_a) \approx -\Phi_a/2$.

Also, as already mentioned in section II, Eqs (19a-b) show that the multiplication of $G(\sigma_v, \delta_e, \sigma_e)$ by any constant has no influence on the relative ratio between the Bessel functions (i.e. between the amplitude of the spectral components of the vibration spectrum). Therefore to restore accurate vibration measurement the frequency shape of the complex gain is important, but not its exact value.

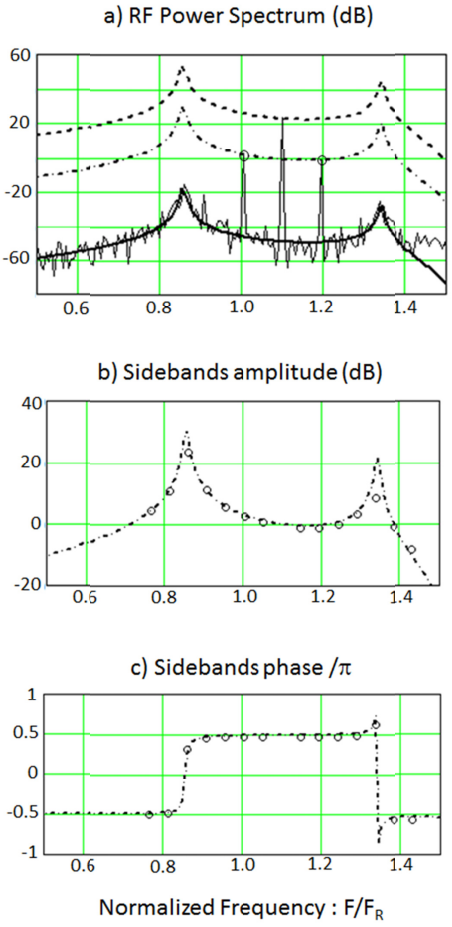

Fig. 4: Numerical simulation. Comparison between the complex amplitude of the vibration sidebands (circle) obtained from a numerical simulation and the non-linear gain (solid, dashed and dash-dotted lines) obtained analytically [Eq. (15)]. a) RF power spectrum of the laser output power modulation for a strong optical feedback ($R_e = 1\times10^{-7}$ and $\Omega_e = 1.1\Omega_R$) and a harmonic vibration ($\Omega_a \approx \Omega_R/10$) with a small amplitude of vibration $\Phi_a = 2\pi/50$. Amplitude (b) and phase (c) of the vibration sidebands, for 7 acoustic frequencies (Ω_a). Laser parameters: see Fig.1.

Fig. 4 shows a comparison between the non-linear gain $G(\sigma_v, \delta_e, \sigma_e)$ given by Eq. (15) and the amplitude of the vibration sidebands (C_e , R_a and L_a) obtained from a numerical simulation. Fig. 4a shows the RF power spectrum of the laser output power modulation for a strong optical feedback ($R_e = 1\times10^{-7}$ and $\Omega_e = 1.1\Omega_R$) and a harmonic vibration ($\Omega_a = \Omega_R/7$) with a small amplitude of vibration $\Phi_a = 2\pi/50$. One can see that the signal is composed of one peak at the carrier frequency (σ_e) and two peaks for the vibration sidebands ($\sigma_e \pm \sigma_a$). The noise power spectrum exhibits a double resonance with resonance frequencies symmetrically located on both sides of the carrier frequency [$\sigma_e \pm \delta_R$].

Also, Fig. 4a allows to show the link among the noise power spectrum, the gain of the laser dynamics and the relative amplitudes of the spectral components of the vibration spectrum. To check the validity of Eqs. (19a-b), the shape (i.e. not the absolute value) of the complex gain is simply determined by adjusting the shape of the analytical expression of $G(\sigma_v, \delta_e, \sigma_e)$ on the noise power spectrum (lower gain curve). In practice, principally the distance and the relative height between the two resonance peaks are carefully adjusted. Then, if the shape of the adjusted gain is renormalized (i.e. multiplied by a constant) to fit the modulation amplitude at the carrier frequency (upper gain curve), the division of the renormalized gain by $J_0(\Phi_a)/J_1(\Phi_a)$, allows to obtain a very good agreement between the value of the gain and the amplitude of the vibration sidebands (middle gain curve).

This verification demonstrates, that the frequency shapes of the complex gain, which must be known [Eq. (4c) or Eqs. (19a-b)] to restore accurate vibration measurement, can be simply determined experimentally by adjusting the shape of $G(\sigma_v, \delta_e, \sigma_e)$ on the shape of the noise power spectrum and whatever the feedback condition (weak or strong) and therefore whatever the laser dynamics (linear or nonlinear).

Figs. 4b and 4c show the amplitude and the phase of the vibration sidebands obtained for different normalized modulation frequencies (σ_a). One can see a very good agreement between the numerical results and the non-linear complex gain $G(\sigma_v, \delta_e, \sigma_e)$ previously determined. This result confirms the possibility to extract quantitative vibration measurements from the non-linear laser dynamics.

4. EXPERIMENTAL RESULTS

A. Experimental setup

To extract quantitative vibration measurements from the non-linear laser dynamics of a laser submitted to frequency shifted optical feedback, we have used a LOFI (Laser Optical Feedback Imaging) setup.

A schematic diagram of this setup is shown in Fig. 5. The laser is a diode pumped Nd:YAG microchip laser. The maximum available pump power is 400 mW at 810 nm and the total output power of the microchip laser is 80 mW with a central wavelength of $\lambda = 1064\,nm$.

The microchip laser has a plane-parallel cavity which is stabilized by the thermal lens induced by the Gaussian pump beam. The two dielectric mirrors are directly coated on the laser material (full cavity). The input dichroic mirror transmits the pump power and totally reflects the infrared laser wavelength. On the other side, the dichroic output mirror allows to totally reflect the pump power (to increase the pump power absorption and therefore the laser efficiency) and only partially reflects (95%) the laser wavelength. The microchip cavity is

relatively short $L_c \approx 1\,mm$ which ensures a high damping rate of the cavity and therefore a good sensitivity to optical feedback.
Part of the light diffracted and/or scattered by the vibrating target returns inside the laser cavity after a second pass through the frequency shifter. Therefore, the optical frequencies of the reinjected light are shifted by F_e. This frequency shift can be adjusted and is typically of the order of the laser relaxation frequency F_R, which is in the megahertz range for the microchip laser used here.
The optical feedback is characterized by the complex target reflectivity ($r_e = \sqrt{R_e}\exp(j\Phi_e)$, where the phase $\Phi_e = \frac{2\pi}{\lambda} 2d_e$ describes the optical phase shift induced by the round trip time delay τ_e (i.e. the distance $d_e = c\,\tau_e$, where c is the velocity of light) between the laser and the target. The effective power reflectivity ($R_e = |r_e|^2$) takes into account the target albedo, the numerical aperture of the collection optics, the frequency shifter efficiency, the transmission of all optical components and the overlap of the retro-diffused field with the Gaussian cavity beam (confocal feature).

To generate vibrations (i.e. a time dependant phase $\Phi_e(t)$), the target is mounted on a Piezo Electric Transducer (PZT) translation stage which allows transient and harmonic displacements with minimum amplitudes in the nanometer range and a maximum frequency of roughly 200 kHz (i.e. $\approx F_R/5$).

Finally, the coherent interaction (beating) between the lasing electric field and the frequency-shifted reinjected field leads to a modulation of the laser output power. For detection purposes, a small part of the laser output beam is sent to a photodiode. The delivered voltage is analysed by a numerical oscilloscope, which allows Fast Fourier Transform (FFT) calculations and processed by a PC to finally obtain quantitative vibration measurements.

One can notice that even if LOFI images can be obtained pixel by pixel by a full 2D galvanometric scanning, only punctual measurements have been made in the present work. Also, one can notice that in comparison with a conventional heterodyne interferometer, the LOFI setup shown here does not require complex alignment. Indeed, the LOFI interferometer is always self-aligned because the laser simultaneously fulfils the functions of the source (i.e. photons-emitter) and the photo-detector (i.e. photons-receptor).

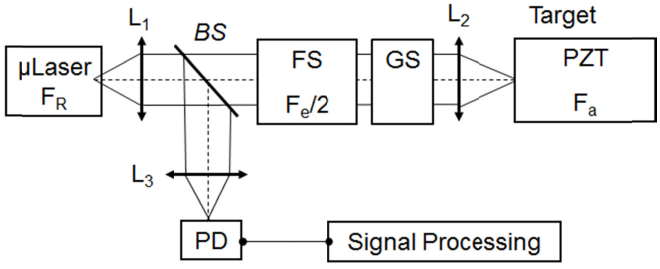

Fig. 5: Schematic diagram of the LOFI setup for vibrometry. µLaser: microchip laser with a relaxation oscillations frequency F_R. L_1, L_2 and L_3: Lenses, BS: Beam Splitter, GS: Galvanometric Scanner, FS Frequency Shifter with a round trip frequency-shift F_e, PZT: Piezo Electric Transducer with a vibration frequency F_a, PD: Photodiode.

B. Measurements of transient harmonic vibrations

To demonstrate that our signal processing can be applied to any kinds of vibrations, we have experimentally measured transient-harmonic vibrations with the LOFI setup (Fig. 6).

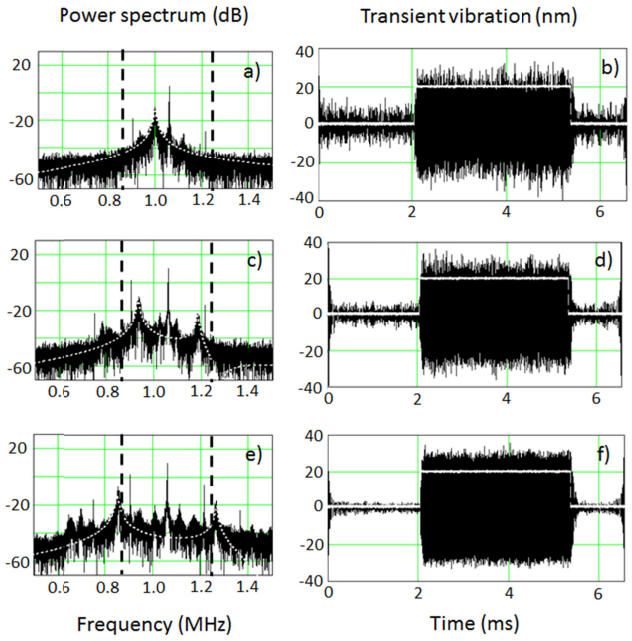

Fig. 6: Experimental results. Detection of a transient-harmonic vibrations with an oscillation frequency of $F_a = 180\,kHz$ (i.e. $F_R/6.5$) and a vibration amplitude $d_a = 28\,nm$. The measurements are made for $F_e = 1.24\,MHz$ ($F_e/F_R \approx 1.1$) and an increasing amount of optical feedback characterized by the laser power impacting the vibrating PZT. Top row (a, b): low feedback ($1.8\,\mu W$); Middle row (c, d): intermediate feedback ($5.6\,\mu W$); Bottom row (e, f): strong feedback($14.9\,\mu W$). The left column (a, c, e) shows the RF power spectra, where the dashed white-lines show the shape of the non-linear gain used for the signal processing. The signal processing is made with a bandpass filter $\Delta F_e = 450\,kHz$ (corresponding to the dashed vertical black-lines). The right column (b, d, f): shows a comparison between the vibration extracted from the signal processing and the time gate when the PZT is triggered (solid white lines).

Experimentally, the laser is set to an output power of 40 mW with a relaxation frequency of $F_R = 1.17\,MHz$ and the carrier frequency (controlled by two AODs) is tuned to $F_e = 1.24\,MHz$ (i.e. $F_e/F_R = 1.06$). Experiments have been made for 3 different amounts of optical feedback. The strength of the optical feedback is controlled by adjusting the conversion efficiency of the two AODs. In Fig. 6 the power of optical feedback is characterized by the laser power impacting the target: $1.8\,\mu W$ for the top row (Figs 6a-b), $5.6\,\mu W$ for the middle row (Figs 6c-d), and $14.9\,\mu W$ for the bottom row (Figs 6e-f). These values correspond to a relative increase of the effective feedback reflectivity (R_e) by a factor of $\times 9.7$ between the first two values and by a factor $\times 7.1$ between the second and the third one.
The transient-harmonic vibration generated by the PZT translation stage is composed of harmonic oscillations with a frequency of

$F_a = 180\,kHz$ (i.e. $F_R/6.5$) within a time gate of $3.3\,ms$ duration (i.e. 600 cycles) starting after a time delay of $2.0\,ms$. The total recording time is $6.6\,ms$ with a sampling rate of $1\times10^7\,samples/s$. For the signal processing, the frequency bandwidth is $\Delta F_e = 450\,kHz$ around F_e.

Fig. 6 shows, that quantitative vibration measurements can be experimentally extracted from the non-linear laser dynamics. The left column shows how the gain is modified when the amount of optical feedback increases (i.e. when $\delta_e \uparrow$). As already mentioned the modification of the non-linear gain is induced by the modification of the carrier amplitude ($C_e(\delta_e, \sigma_e)$). Starting with a linear gain (Fig. 6a), the gain becomes more and more non-linear when $\delta_e \uparrow$ (Figs. 6b-c). In agreement with Eq. (16a), one can observe for the non-linear gain (Figs 6c and 6e) that the frequency distance between the two maxima (located symmetrically on both sides of the carrier frequency) increases. Secondly, in agreement with Eq. (16b), one can also observe that the amplitude of the maximum located on the right side of the carrier frequency increases.
The left column allows to show that the modulation amplitude at the carrier frequency can saturate when the optical feedback becomes too strong. Indeed, Figs. 6c and 6e show a roughly constant amplitude of the carrier, although the amount of optical feedback is increased ($\times7.1$).
Despite this saturation, the right column of Fig. 6 shows that regardless of the shape of the gain (i.e. linear or non-linear) the transient-harmonic vibration is recovered with an accurate time delay, characterized by the trigger trace superimposed. It should be noted that the presented time traces are an average on ten acquisitions. By looking more precisely near the rising and falling edges, one can also observe the transient time response of the PZT.

When the amount of optical feedback increases, one can observe a small increase of the mean value of the stationary vibration amplitude ($21\,nm$, $25\,nm$ and $28\,nm$), while one can observe a small decrease of the vibration noise ($6\,nm$, $3\,nm$ and $1\,nm$). The amplitude of the vibration noise has been determined during the starting time delay (i.e. before the starting of the harmonic vibrations). For a given detection bandwidth, this reduction of the vibration noise could be qualitatively explained by the increase of the carrier signal, coupled simultaneously with a modification of the laser noise power spectrum induced by the optical feedback, in the vibration frequency range.

For comparison, the vibration amplitude value measured at low frequency (150 Hz) with a lock-in amplifier gives $28\,nm$. So, taking into account the noise, the obtained results are in relative good agreement and one can notice that the better value is obtained for the strongest feedback ($28\pm1\,nm$) where the non-linear gain compensation is necessary.

5. CONCLUSIONS AND PERSPECTIVES

The main motivation of this study is the understanding of the non-linear response of a LOFI sensor for quantitative phase measurements of small vibrations. The use of a LOFI set up is motivated by the following reasons: i) the LOFI interferometer is always self-aligned because the laser simultaneously fulfils the functions of the source (i.e. photons-emitter) and of the photo-detector (i.e. photons-receptor); ii) the LOFI detection is shot noise limited (even with a low power laser) in a frequency range located near the relaxation oscillation frequency of the laser.
For small vibrations, the amplitude of the modulation at the carrier frequency is several order of magnitude higher than the amplitude of vibration sidebands at the acoustic frequency. Consequently, the optical feedback needs to be strong to be able to observe the small vibration sidebands and under these conditions the laser dynamics becomes non-linear. In this paper we have demonstrated (analytically, numerically and experimentally) how quantitative vibration measurements (harmonic or transient) can be extracted from the non-linear dynamics of a laser submitted to frequency shifted optical feedback. By using a multiscale analysis, we have analytically studied the non-linear dynamics of a laser subjected to frequency shifted optical reinjection coming back from a vibrating target. More specifically, we have studied the non-linear dynamical coupling between the modulation at the carrier frequency and the modulation of the vibration sidebands at the acoustic frequency. We have shown how the non-linear amplification of the vibration spectrum by the laser dynamics is related to the strength of the optical feedback (and therefore of the amplitude of the carrier) and how it can be compensated to obtain accurate (i.e. without bias) vibration measurements in the nanometer range at relatively high frequency (of the order of several hundred of kHz). The theoretical predictions, confirmed by numerical simulations, are in good agreement with the experimental data for both transient and harmonic vibrations.
Of course, the compensation effect is more important and therefore more necessary when the vibration spectrum is in the vicinity of the resonance frequency of the laser dynamics and therefore is strongly deformed. This nearly resonant situation corresponds to the conventional use of a LOFI setup to obtain a shot noise limited detection of the optical feedback.
Encouraged by these preliminary results, the sensitivity and performances of the non-linear LOFI device will be tested (in a near future) for the optical detection (with a shot-noise sensitivity) of acoustics waves induced by a photo-acoustic effect [27, 28].

References

1. R. Lang and K. Kobayashi, "External optical feedback effects on semiconductor injection laser properties ," IEEE J. Quantum Electron. **QE-16**, 347-355 (1980).
2. T. Erneux, V. Kovanics, and A. Gavrielides, "Non-linear dynamics of an injected quantum cascade laser," Phys. Rev. E **88**, 032907 (2013).
3. T. Taimre, M. Nikolic, K. Bertling, Y. L. Lim, T. Bosch and A. D. Rakic,"Laser feedback interferometry: a tutorial on the self-mixing effect for coherent sensing," Adv. in Opt. and Photon. **7**, 570,631 (2015)
4. K. Otsuka, "Effects of external perturbations on $LiNdP_4O_{12}$ Lasers," IEEE J. Quantum Electron., **QE-15**, 655-663 (1979).
5. K. Otsuka, "Self-Mixing Thin-Slice Solids-State Laser Metrology," Sensors **11**, 2195-2245 (2011).
6. S. Okamoto, H. Takeda, and F. Kannari, "Ultrahighly sensitive laser-Doppler velocity meter with a diode-pumped Nd:YVO4 microchip laser," Rev. Sci. Instrum. **66,** 3116–3120 (1995).
7. R. Kawai, Y. Asakawa, K. Otsuka, "Ultrahigh-Sensitivity Self-Mixing Laser Doppler Velocimetry with Laser-Diode-Pumped Microchip $LiNdP_4O_{12}$ Lasers," IEEE Photonics Technology Lett. **11**, 706-708 (1999).
8. S. Suddo, T. Ohtomo, Y. Takahascvhi, T. Oishi, K. Otsuka, "Determination of velocity of self-mobile phytoplankton using a self thin-slice solid–state laser," Appl. Opt. **48**, 4049-4055 (2009).
9. E. Lacot, R. Day, and F. Stoeckel, "Laser optical feedback tomography," Opt. Lett. **24,** 744–746 (1999).
10. O. Hugon, F. Joud, E. Lacot, O. Jacquin, H. Guillet de Chatellus, "Coherent microscopy by laser optical feedback imaging (LOFI)

technique," Ultramicroscopy (2011) doi: 10.1016/j.ultramic.2011.08.004.
11. W. Glastre, O. Hugon, O. Jacquin, H. Guillet de CHatellus, and E. Lacot, "Demonstration of a plenoptic microscope based on laser optical feedback imaging," Opt. Exp. **21,** 7294–7303 (2013).
12. E. Lacot, R. Day, "Coherent laser detection by frequency-shifted optical feedback," Phys. Rev. A **64**, 043815 (2001).
13. E. Lacot, O. Jacquin, G. Roussely, O. Hugon, H. Guillet de Chatellus, "Comparative study of autodyne and heterodyne laser interferometry for imaging," J. Opt. Soc. Am. A **27**, 2450-2458 (2010).
14. O. Jacquin, E. Lacot, W. Glastre, O. Hugon, H. Guillet de Chatellus, "Experimental comparison of autodyne and heterodyne laser interferometry using an Nd:YVO4 microchip laser," J. Opt. Soc. Am. A **28**, 1741-1746 (2011).
15. K. Otsuka, K. Abe, J.Y. Ko, and T.S. Lim, "Real-time nanometer vibration measurement with self-mixing microchip solid-state laser," Opt. Lett. **27**, 1339-1341 (2002).
16. E. Lacot, O. Hugon, "Phase-sensitive laser detection by frequency-shifted optical feedback," Phys. Rev. A **70**, 053824 (2004).
17. V. Muzet, E.Lacot, O. Hugon, Y. Gaillard, "Experimental comparison of shearography and laser optical feedback imaging for crack detection in concrete structures," Proc. SPIE 5856, 793-799 (2005).
18. K. Peterman, Laser diode modulation and noise (Springer, 1988)
19. M.I. Kolobov, L. Davidovitch, E. Giacobino, and C. Fabre, "Role of pumping statistics and dynamics of atomic polarization in quantum fluctuations of laser sources," Phys. Rev. A **47**, 1431-1446 (1993).
20. Y. Tan, C. Xu, S. Zhang, and S. Zhang, "Power spectral characteristic of a microchip Nd:YAG laser subjected to frequency-shifted optical feedback," Laser Phys. Lett. **10**, 025001 (2013).
21. Y. Tan, S. Zhang, S. Zhang, Y. Zhang and N. Liu, "Response of microchip solid state laser to external frequency-shifted feedback and its applications," Sci. Rep. **3**, 2912 (2013).
22. E. Lacot, B. Houchmandzadeh, V. Girardeau, O. Hugon, O. Jacquin, "Non linear modification of the laser noise power spectrum induced by frequency-shifted optical feedback," Accepted, Phys. Rev. A (2016).
23. I. B. Schwartz and T. Erneux,"Subharmonic hysteresis and period doubling bifurcations for periodically driven laser," SIAM J. Appl. Math **54**, 1083-1100 (1994).
24. A. Witomski, E. Lacot, O.Hugon, T. Erneux, "Parametric amplification of frequency-shifted optical feedback," Phys. Rev. A **72**, 023801 (2005).
25. M.W. Phillps, H. Gong, A.I. Ferguson, and D.C. Hanna,"Optical Chaos and hystetresis in a laser-diode pumped Nd doped fibre laser," Opt. Comm. **61**, 215-218 (1987).
26. J.C. Celet, D. Dangoisse, P. Glorieux, G. Lythe and T. Erneux, "Slowly passing through resonance strongly depends on Noise," Phys. Rev. Lett. **81**, 975-978 (1998).
27. C. Li and L.V. Wang, "Photoacoustic tomography and sensing in biomedicine," Phys. Med. Biol. **54**, R54-R97 (2009).
28. S. A. Carp and V. Venugopalan,"Optoacoustic imaging based on the interferometric measurement of surface displacement," J. of Biomed. Opt. **12**, 064001 (2007).